

Research article

Two new Asian species of *Russula* sect. *Ingratae* with unique basidiospore features for subg. *Heterophyllidiae*Aniket GHOSH¹, Bart BUYCK², Kanad DAS³,
Ishika BERA⁴ & Dyutiparna CHAKRABORTY^{5,*}¹Cryptogamic Unit, Central National Herbarium, Botanical Survey of India,
3rd MSO Building DF block, Sector 1, Salt Lake City, Kolkata – 700064, India.²Institut de Systématique, Evolution, Biodiversité (ISYEB), Muséum national d'histoire naturelle,
CNRS, Sorbonne Université, EPHE, Université des Antilles CP 39,
57 rue Cuvier, 75005 Paris, France.^{3,4}Central National Herbarium, Botanical Survey of India, P.O. – Botanic Garden,
Howrah – 711103, India.⁵Eastern Regional Center, Botanical Survey of India, Shillong – 793003, India.* Corresponding author: dyuti.parna.mail@gmail.com¹ Email: ghosh.aniket87@gmail.com² Email: buyck@mnhn.fr³ Email: daskanadbsi@gmail.com⁴ Email: iamishika6@gmail.com

Abstract. Two novel species of *Russula* (Russulaceae, Russulales), namely *Russula indosenecis* A.Ghosh, D.Chakr., K.Das & Buyck sp. nov. and *R. pseudosenecis* A.Ghosh, D.Chakr., K.Das & Buyck sp. nov. belonging to sect. *Ingratae* subg. *Heterophyllidiae* are proposed herein based on their morphological features and nrITS-based phylogenetic inferences. Both species belong to the Asian '*R. punctipes-senecis*' complex of sect. *Ingratae*. The acrid *R. indosenecis* was collected from subalpine forests associated with *Abies densa*, whereas the mild *R. pseudosenecis* associates with tropical forests dominated by *Shorea robusta*. Both species are distinct from the other species of this species complex in nrITS sequence data and from all other known species in subg. *Heterophyllidiae* in the strong amyloidity of their suprahilar spot.

Keywords. Macrofungi, nrITS, phylogeny, Russulales, taxonomy.

Ghosh A., Buyck B., Das K., Bera I. & Chakraborty D. 2022. Two new Asian species of *Russula* sect. *Ingratae* with unique basidiospore features for subg. *Heterophyllidiae*. *European Journal of Taxonomy* 847: 104–120. <https://doi.org/10.5852/ejt.2022.847.1985>

Introduction

Russula Pers. has a nearly cosmopolitan distribution with species occurring from tropical to arctic ecosystems where they form symbiotic relationships with a diversity of plant species in broad-leaved and coniferous forests, scrubland and meadows (Adamčík *et al.* 2019; Hackel *et al.* 2022). Agaricoid

members of this genus frequently have a colourful fragile pileus, amyloid spore ornamentation, a brittle context with abundant sphaerocytes and presence of gloeoplerous elements in various parts of their fruiting bodies, but they lack a branching lactiferous system ending in pseudocystidia at the basidiome surface as in the genera *Lactarius* Pers. and *Lactifluus* (Pers.) Roussel (Buyck *et al.* 2018). Recently, Buyck *et al.* (2018) demonstrated that the anatomy of ectomycorrhiza added support to a new infrageneric classification system of *Russula* based on a new multi-locus analysis (LSU, mtSSU, *rpb2*, *rpb1* and *tef-1*), which was followed in this study.

During extensive macrofungal forays in subalpine Arunachal Pradesh and tropical forests of West Bengal and Jharkhand, a number of interesting specimens of genus *Russula* were collected that appeared affiliated to *Russula* sect. *Ingratae* Qué. based on morphology and nBLAST top scores. Species belonging to *Russula* sect. *Ingratae* are mostly characterized by having a tawny, ochraceous or ashy-gray to dark brown coloured pileus with tuberculate striate margin, equal lamellae sometimes forked or intermixed with few lamellulae, a mild to very acrid taste and often producing a strong disagreeable or very sweet smell (fetid, spermatic, waxy or like bitter almonds); they produce cream-coloured spore prints and basidiospores that have an inamyloid or partly amyloid suprahilar area; they have abundant gloeoplerous elements throughout their tissues and small, often mucronate, unicellular pileocystidia at the pileus surface mixed with branched, short-celled hyphal ends in the pileipellis (Singer 1986; Samari 1998). The combination of these characters makes section *Ingratae* one of the more easily distinguishable groups in subgenus *Heterophyllidiae* Romagn. and it forms a well-supported, monophyletic lineage in recently published ITS (Li *et al.* 2021) and multi-gene (Buyck *et al.* 2018; Chen *et al.* 2021; Han *et al.* 2022; Song *et al.* 2018) phylogenetic analyses.

Thirty new species of sect. *Ingratae* have already been described from Asia and, with few exceptions, nearly all in the past twenty years, including eight from India: *R. abbotensis* K.Das & J.R.Sharma, *R. arunii* Paloi, A.K.Dutta & K.Acharya, *R. benghalensis* S.Paloi & K.Acharya, *R. dubdiana* K.Das, Atri & Buyck, *R. indocatillus* A.Ghosh, K.Das & R.P.Bhatt, *R. natarajanii* K.Das, J.R.Sharma & Atri, *R. obscuricolor* K.Das, A.Ghosh & Buyck and *R. tsokae* K.Das, Van de Putte & Buyck (Das *et al.* 2006; 2010, 2017; Crous *et al.* 2017; Ghosh *et al.* 2020; Yuan *et al.* 2020)

Detailed morphological examinations and molecular phylogenetic analyses of our recent collections revealed two undescribed species of sect. *Ingratae*, which are presented here as *R. indosenecis* sp. nov. and *R. pseudosenecis* sp. nov., respectively. Both novel species are supported by phylogenetic analysis based on nrITS sequences. Detailed macro- and micromorphological descriptions coupled with illustrations are provided for both and comparisons with closely related species are discussed.

Materials and methods

Morphology

Fresh specimens were macromorphologically described and images of the basidiomata were taken with a Sony DSC-WX500 and Canon Power Shot SX 50 HS. Colours were coded using the *Methuen Handbook of Colour* (Kornerup & Wanscher 1978). The specimens were then dried with a field drier. Micromorphological studies are after Adamčík *et al.* (2019) and Ghosh *et al.* (2021). The adopted terminology used to describe the morphology and anatomy of microscopic cells and tissues followed Vellinga (1988). Drawings of micromorphological features were made with a drawing tube attached to an Olympus CX 41 at 1000× magnification. Microscopic photographs were taken with an Olympus BX 53 camera. Basidiospores were examined in Melzer's reagent and measured in side view, excluding ornamentations. Scanning electron microscope (SEM) images of basidiospores were made from dry spores that were directly mounted on a double-sided adhesive tape pasted on a metallic specimen-stub and then scanned with silver coating at different magnifications in high vacuum mode (20 KV) to observe patterns of spore-ornamentation. SEM work was carried out with a ZEISS EVO 18 SPECIAL EDITION model imported from Germany and installed at USIC Dept., HNBGU Srinagar (Garhwal) India. Specimens were deposited at Central National Herbarium (CAL), Howrah.

DNA extraction, polymerase chain reaction (PCR) and sequencing

Genomic DNA was extracted from 100 mg of dried basidiome (for two species) with the InstaGene™ Matrix Genomic DNA isolation kit (Biorad, USA) following the manufacturer's instructions. The internal transcribed spacer (ITS) region of ribosomal DNA was amplified with primer pairs ITS1-F and ITS4 (White *et al.* 1990; Gardes & Bruns 1993). PCR protocol for the amplification of ITS regions followed Ghosh *et al.* (2021). The PCR products were purified using the QIAquick PCR Purification Kit (QIAGEN, Germany). Both strands of the PCR fragment were sequenced on the 3730xl DNA Analyzer (Applied Biosystems, USA) using the amplifying primers. The sequence quality was checked using Sequence Scanner Software ver. 1 (Applied Biosystems). Sequence alignment and required editing of the obtained sequences were carried out using Geneious ver. 5.1 (Drummond *et al.* 2010). The final consensus sequences were deposited at GenBank to procure the accession numbers: OL701269 and OL701254 for *R. indosenecis* sp. nov., OL461233 and OL461234 for *R. pseudosenecis* sp. nov.

Phylogenetic analysis

The newly generated nrITS sequences of the two species of *Russula* (*Russula indosenecis* sp. nov., and *R. pseudosenecis* sp. nov.) and their close relatives retrieved from nBLAST searches against GenBank (<https://www.ncbi.nlm.nih.gov/genbank>), UNITE database (Kõljalg *et al.* 2013) and relevant published phylogenies (Song *et al.* 2018; Yuan *et al.* 2020), were aligned using the online version (<https://mafft.cbrc.jp/alignment/software/>) of the multiple sequence alignment program MAFFT ver. 7, with the E-INS-i strategy (Katoh *et al.* 2019). The aligned sequences were trimmed with the conserved motifs 5'-(...aaggat)catta... and ...ttgacct(caaa...)-3'. The single-locus dataset was phylogenetically analyzed using both maximum likelihood (ML) and Bayesian inference (BI) methods. ML was performed using raxmlGUI 2.0 (Edler *et al.* 2021) with the GTRGAMMA substitution model. ML analysis was executed applying the rapid bootstrap algorithm with 1000 replicates to obtain nodal support values. For BI, ITS alignments were divided into three partitions: ITS1, 5.8S and ITS2. PartitionFinder2 was used to find the best substitution models (GTR+G for ITS1 and ITS2; SYM+G for 5.8S) using the Akaike information criterion (AICc) with a greedy search over all models (Lanfear *et al.* 2017). BI was computed in MrBayes ver. 3.2.6 (Ronquist *et al.* 2012) with four Markov chain Monte Carlo (MCMC) chains for 1 000 000 iterations until the standard deviation of split frequencies reached below the 0.01 threshold. Trees were sampled every 100th generation. The first 25% of trees were discarded as burn-in. Chain convergence was determined using Tracer ver. 1.6 (Rambaut *et al.* 2014) to ensure sufficiently large effective sample size (ESS) values (>200). Gaps in the alignment were treated as missing data in phylogenetic analyses. Maximum likelihood bootstrap (MLbs) values $\geq 70\%$ and Bayesian posterior probabilities (BPP) values ≥ 0.95 are shown in the phylogenetic tree (Fig. 1).

Results

Molecular phylogeny

The final dataset consisted of 69 nrITS sequences. The final alignment comprised 741 characters including gaps. The obtained phylogenetic tree (showing two novel species in bold red font) is presented in Fig. 1.

Our nrITS-based phylogeny (Fig. 1) obtained full support (MLbs = 100%, BPP = 1) to place both newly sequenced species as monophyletic lineages within a larger clade that is here referred to as the '*R. punctipes-senecis*' complex. The latter clade received equally strong support (MLbs = 99%, BPP = 1) and is placed sister without support to the recently described, Indian *R. benghalensis*. Whereas sequences obtained from *R. pseudosenecis* sp. nov. (GenBank accession numbers: OL461233 and OL461234) are nested within the '*R. punctipes-senecis*' clade, sequences of *R. indosenecis* sp. nov. (GenBank accession numbers: OL701269 and OL701254) are placed, although without support, on a short branch that is sister to the remainder of the Asian '*R. punctipes-senecis*' complex.

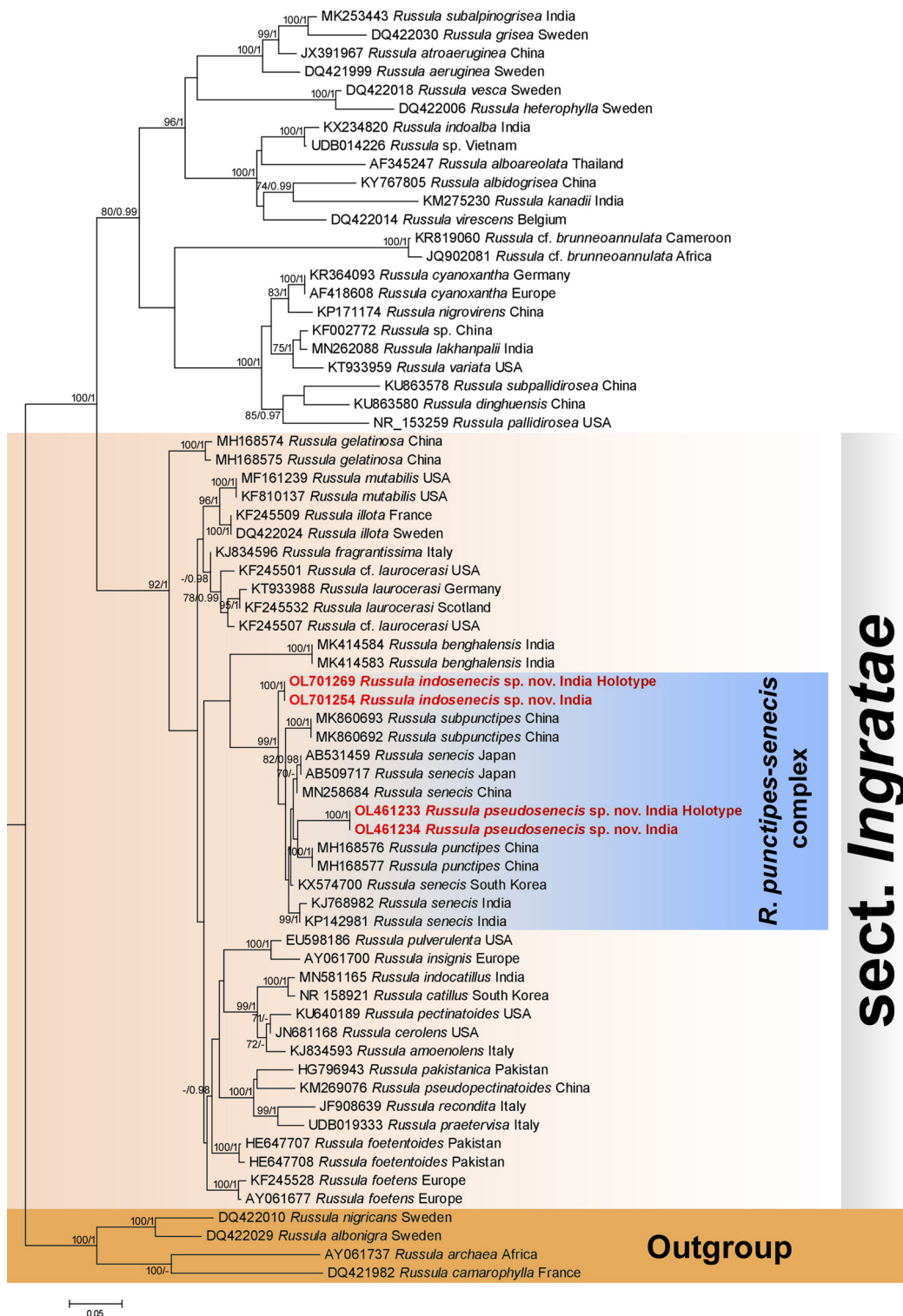


Fig. 1. Phylogram generated by maximum likelihood analysis based on sequence data of nrITS for *Russula indosenecis* A.Ghosh, D.Chakr., K.Das & Buyck sp. nov. and *R. pseudosenecis* A.Ghosh, D.Chakr., K.Das & Buyck sp. nov. and their allied species. Maximum likelihood bootstrap support values (MLBs) $\geq 70\%$ are shown on the left of '/' and Bayesian posterior probabilities (BPP) ≥ 0.95 are shown on the right above or below the branches at nodes. *R. indosenecis* sp. nov. and *R. pseudosenecis* sp. nov. are placed in bold red font to highlight their phylogenetic positions in the tree.

Taxonomic treatments

Phylum Basidiomycota R.T.Moore
Class Agaricomycetes Doweld
Order Russulales Kreisel ex P.M.Kirk, P.F.Cannon & J.C.David
Family Russulaceae Lotsy
Genus *Russula* Pers.

Russula indosenecis A.Ghosh, D.Chakr., K.Das & Buyck sp. nov.
Mycobank: [MB842307](#)
Figs 2–4A

Diagnosis

Russula indosenecis sp. nov. resembles Japanese *R. senecis* Imai but differs from it mainly by the strongly amyloid suprahilar spot on the basidiospores, genetic distance of the nrITS sequences (97.25%–97.79% similarity) and its occurrence under *Abies densa* Giff. in subalpine forests.

Etymology

Referred to its occurrence in Indian Himalaya and morphological resemblance to *R. senecis*.

Material examined

Holotype

INDIA • East Himalayan Region, Tawang district, on the way to Panga Teng Tso Lake; 27°38'15.5" N, 91°51'12.1" E; alt. 3935 m a.s.l.; in subalpine forest under *Abies densa*; 30 Aug. 2021; A. Ghosh AG-21-06A; GenBank: OL701269 (ITS); CAL[1856].

Paratype

INDIA • East Himalayan Region, Tawang district, on the way to Panga Teng Tso Lake; 27°38'15.2" N, 91°51'11.6" E; alt. 3919 m a.s.l.; in subalpine forest under *Abies densa*; 29 Aug. 2021; A. Ghosh AG-21-04A; GenBank: OL701254 (ITS); CAL[1857].

Description

Pileus medium to large sized, 65–140 mm in diameter, convex, planoconvex to applanate with broadly depressed center, becoming infundibuliform with maturity; margin decurved to plane or uplifted with maturity, entire, strongly tuberculate-striate; surface viscid and glutinous when moist, dull with drying, quickly cracked, easily peeled off $\frac{1}{3}$ rd to $\frac{3}{4}$ th toward center, light orange or melon yellow or apricot yellow or golden yellow (5A–B5–7), centrally turning dark brown (6–7E6–8) with maturity or age, turning orange (6A8) with KOH. Pileus context up to 6 mm thick at the disc, compact, brittle, firm, chalky white (1–2A1), unchanging after bruising or on exposure. Lamellae shortly adnate to subfree, equal or with rare lamellulae, subdistant (7–10/cm at pileus margin), rarely forked, chalky white (1A1) to pale cream (3A2) when young, becoming concolorous to pileus colour with age or maturity, unchanging after bruising or on exposure; edges punctuated with brownish orange (6C5–7) or light brown (6D5–7), entire. Stipe long and slender, 90–160 × 13–30 mm, firm, brittle, cylindrical to subclavate, centrally attached; surface dry, smooth, longitudinally striate, light yellow to maize yellow (4A4–6) with light brown (6D5–7) to brown (6D6–7) tinges. Stipe context light orange or apricot yellow or golden yellow (5A–B5–7), multi-chambered, soon hollowing, unchanging on exposure; turning deep to dark turquoise (24E–F7–8) with guaiacol, insensitive to FeSO₄. Odor indistinctive. Taste acrid and very strong to hurting. Spore print pale cream (Iib).



Fig. 2. *Russula indosenecis* A.Ghosh, D.Chakr., K.Das & Buyck sp. nov. (from holotype, AG-21-06A). A–C. Fresh and dissected basidiomata in the field and basecamp. D–E. Transverse section through pileipellis showing elements. F–H. Transverse section through lamellae showing hymenial cystidia near the lamellae sides. I. Transverse section through lamellae showing hymenial cystidia near the lamellae edges. J. Transverse section through lamellae showing hymenial cystidia near the lamellae sides and basidia. K. SEM micrograph of basidiospores. Scale bars: A–B = 50 mm; D–E = 20 μ m; F–J = 10 μ m; K = 2 μ m.

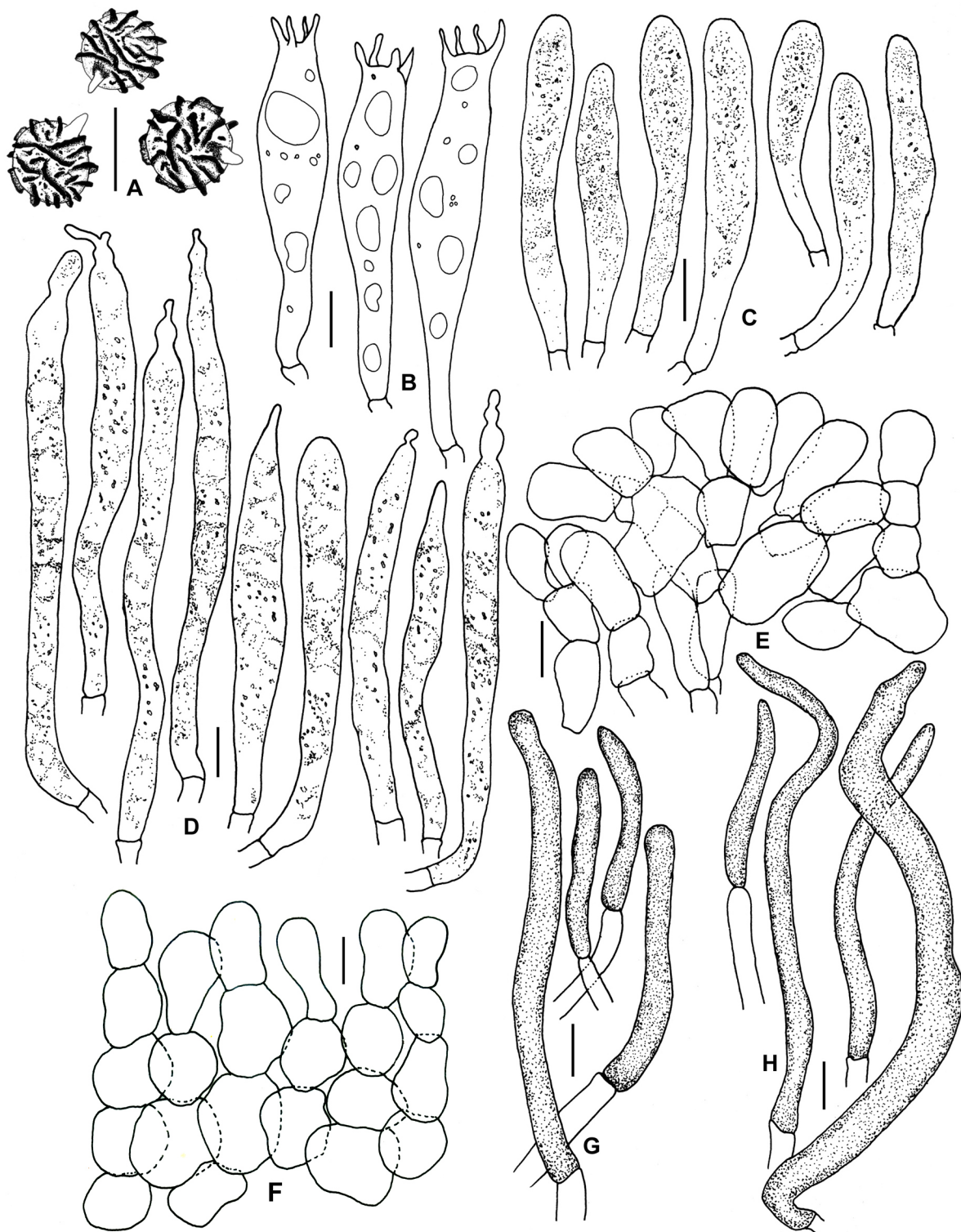


Fig. 3. *Russula indosenecis* A.Ghosh, D.Chakr., K.Das & Buyck sp. nov. (from holotype, AG-21-06A). A. Basidiospores. B. Basidia. C. Hymenial cystidia near the lamellae edges. D. Hymenial cystidia on lamellae sides. E, G. Elements of the pileipellis near the pileus margin: hyphal terminations and pileocystidia. F, H. Elements of the pileipellis near the pileus center: hyphal terminations and pileocystidia. Scale bars: A–H = 10 μ m.

Basidiospores globose to subglobose, (8.4–)8.8–9.3–9.8(–10.5) × (8.2–)8.6–9.0–9.5(–10.4) μm, Q = (1–)1.01–1.03–1.06(–1.10); ornamentation amyloid, composed of up to 1.8 μm high wings running over more or less long distances on the spore surface or even nearly encircling the spores, mixed with dense, low network of short, laterally flattened, blunt ridges and warts forming an incomplete network, intermixed with crowded, isolated warts and large spines (up to 1.5 μm high), some spines partly connected; suprahilar spot indistinct, warted, sometimes partially amyloid; apiculi up to 2.7 μm long. Basidia (52–)58–64–71(–75) × 11–13–14(–15) μm, 4-spored, subclavate to clavate, tapered at the base; sterigmata up to 6 μm long. Hymenial cystidia on lamellae sides (68–)73.9–85.7–97.5(–115) × 5.5–8–10.5(–16) μm, abundant, cylindrical to lanceolate with obtuse-rounded, mucronate to capitate or subcapitate, appendiculate to lageniform or moniliform apex, emergent up to 50 μm beyond the basidiole tips, few deeply embedded; content dense, finely crystalline with refractive granular bodies, turning gray-black with sulfovanillin. Lamellae edges fertile with basidia and cystidia. Hymenial cystidia on lamellae edges (37–)44.7–51.5–58 × (6–)6.8–7.5–8 μm, cylindrical to lanceolate with obtuse-rounded apex; content dense, finely crystalline with refractive granular bodies, turning gray-black with sulfovanillin. Marginal cells not differentiated. Subhymenium layer up to 35 μm thick, pseudoparenchymatous. Hymenophoral trama composed mainly of large nests of sphaerocytes and few hyphal elements. Pileipellis orthochromatic in Cresyl Blue, sharply delimited from the underlying sphaerocytes of the context, 140–150 μm thick, two-layered; subpellis 65–70 μm deep, composed of more or less densely intermixed, horizontally oriented hyphae and dispersed pileocystidia; suprapellis pseudoparenchymatous, an ixo-palisade, 75–80 μm thick, mainly composed of ascending to erect, densely septate hyphal extremities forming chains of mostly strongly inflated cells. Acidoresistant incrustations absent. Hyphal terminations near the pileus margin thin-walled, composed of chains of 3–5 cells, sometimes branched at the terminal cells; terminal cells (12–)13.9–20.6–27.3(–42) × 7–10.1–12.9(–19) μm, mainly clavate to subglobose or cylindrical with rounded apex; subterminal cells inflated or cylindrical. Hyphal terminations in the pileus center also thin-walled, rarely branched at the subterminal cells; terminal cells measuring (11–)14.3–19.9–25.5(–36) × 6–9.1–12.2(–18) μm, mainly cylindrical or clavate; subterminal cells mainly cylindrical or inflated. Pileocystidia near the pileus margin single celled, long, flexuous, thin-walled, (40–)35.1–57.3–79.4(–104) × 5–6.1–7.2(–8) μm, mainly cylindrical, apically mainly obtuse-rounded; contents finely crystalline with refractive granular bodies, turning gray-black in sulfovanillin. Pileocystidia near the pileus center similar, but comparatively longer and broader, (42–)60–92.3–124(–140) × (5–)4.6–6.6–8.7(–10) μm, and sometimes with lateral projections. Oleiferous hyphae present in pileus context. Clamp connections absent from all tissues.

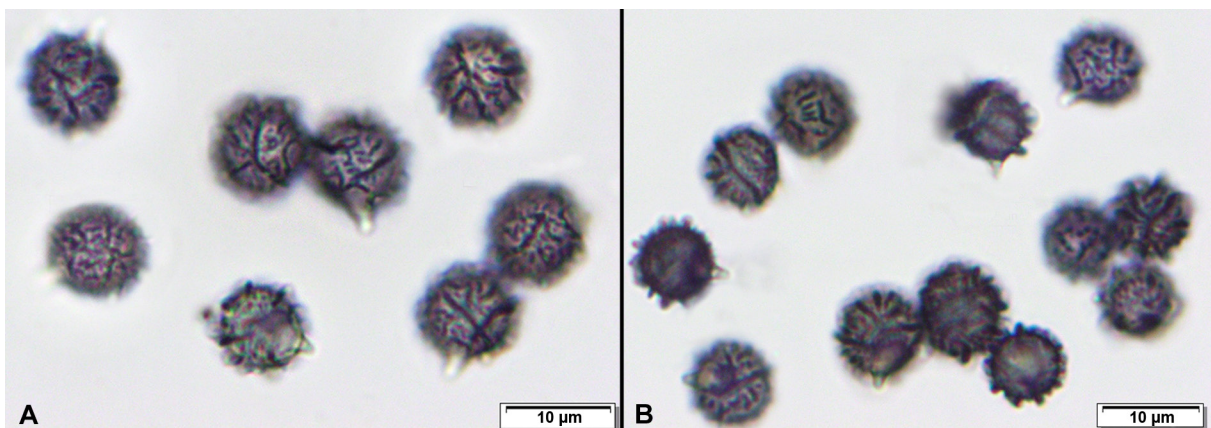


Fig. 4. Basidiospores in Melzer's reagent. **A.** Basidiospores of *Russula indosenecis* A.Ghosh, D.Chakr., K.Das & Buyck sp. nov. **B.** Basidiospores of *Russula pseudosenecis* A.Ghosh, D.Chakr., K.Das & Buyck sp. nov.

Russula pseudosenecis A.Ghosh, D.Chakr., K.Das & Buyck sp. nov.

Mycobank: [MB842137](#)

Figs 4B–6

Diagnosis

Russula pseudosenecis sp. nov. differs mainly from *R. senecis* Imai by its mild taste, paler pileus colour, chalky white gills when young, strongly amyloid suprahilar spot on the basidiospores and its association with *Shorea robusta* C.F.Gaertn. from the tropical tree family Dipterocarpaceae Blume.

Etymology

Referring to it being a look-alike of *R. senecis*, originally described from Japan.

Material examined

Holotype

INDIA • West Bengal, Bankura district, Joypur forest; 23°03'11" N, 87°25'49" E; alt. 74 m a.s.l.; in tropical forest under *Shorea robusta*; 30 Aug. 2020; *A. Ghosh AG 20-062*; GenBank: OL461233 (ITS); CAL[1858].

Additional material

INDIA • West Bengal, Paschim Medinipur district, Chandra; 22°21'01" N, 87°02'00" E; alt. 90 m a.s.l.; in tropical forest under *Shorea robusta*; 12 Aug. 2020; *A. Ghosh AG 20-019*; CAL[1895] • Jhargram district, Tuluha; 22°19'44" N, 87°02'39" E; alt. 80 m a.s.l.; in tropical forest under *Shorea robusta*; 11 Aug. 2021; *A. Ghosh AG 21-073*; GenBank: OL461234 (ITS); CAL[1859] • Uttar Dinajpur, Kaliyaganj, Dhamja forest; 25°34'56" N, 88°20'16" E; alt. 80 m a.s.l.; in tropical forest under *Shorea robusta*; 10 Oct. 2021; *D. Chakraborty, RGJ-20-04*; CAL[1896] • Jharkhand, Rajmahal hills, Pakur district, Hiranpur block, Talpahari to Tugutola forest area; 24°37'02.6" N, 87°40'45.2" E; alt. 94 m a.s.l.; in tropical forest under *Shorea robusta*; 26 Aug. 2021; *A. Ghosh AG 21-14 (JH)*; CAL[1897] • *ibid.*, Sahibganj district, Borio block, Dhogada, Paharia burial ground forest; 25°02'23.7" N, 87°39'35.8" E; alt. 110 m a.s.l.; in tropical forest under *Shorea robusta*; 17 Sep. 2022; *A. Ghosh AGJH-033*; CAL [1898].

Description

Pileus small to medium-sized, 15–55 mm in diameter, convex, planoconvex to applanate with depressed center; margin decurved to plane, entire, strongly tuberculate-striate; surface viscid and glutinous when moist, dull upon drying, quickly cracked, easily peeled off $\frac{1}{3}$ rd to $\frac{1}{2}$ th towards center with maturity, pale yellow, light yellow to grayish yellow (4A–B3–5) or yellowish brown, light brown to golden brown (5D–E5–8), centrally dark brown (6–7E6–8) with maturity or age. Pileus context up to 5 mm thick at the disc, compact, firm, chalky white (1–2A1), unchanging after bruising or on exposure. Lamellae adnate to adnexed, close to crowded (12–15/cm at pileus margin), up to 4 mm thick, chalky white (1–2A1), entire, forked at the stipe apex, middle and near the margin, unchanging after bruising or on exposure; edges punctuated with brownish orange (6C5–7) or light brown (6D5–7), entire; lamellulae rare. Stipe 20–45 × 9–15 mm, firm, brittle, cylindrical to subclavate, centrally attached; surface dry, longitudinally striate, pale to light yellow (4A3–4) or grayish yellow (4B5–6) with light brown (6D5–7) to brown (6D6–7) tinges, unchanging when bruised or on exposure; turning salmon pink (6A4) and deep to dark turquoise (24E–F7–8) in FeSO₄ and guaiacol, respectively. Stipe context pale yellow to light yellow (5A3–5), chambered, unchanging when bruised or on exposure; turning salmon pink (6A4) and deep to dark turquoise (24E–F7–8) in FeSO₄ and guaiacol, respectively. Odor indistinctive. Taste mild. Spore print not observed.



Fig. 5. *Russula pseudosenecis* A.Ghosh, D.Chakr., K.Das & Buyck sp. nov. (from holotype, AG 20-062). A–C. Fresh and dissected basidiomata in the field and basecamp. D–F. Transverse section through pileipellis showing elements. G. Transverse section through lamellae showing basidia. H. Transverse section through lamellae showing hymenial cystidia near the lamellae edges. I–K. Transverse section through lamellae showing hymenial cystidia near the lamellae sides. L. SEM micrograph of basidiospores showing the uplifted (and thus strongly amyloid) suprahilar plage. Scale bars: A–C = 30 mm; D, H = 20 μ m; E–G, I–K = 10 μ m; L = 2 μ m.

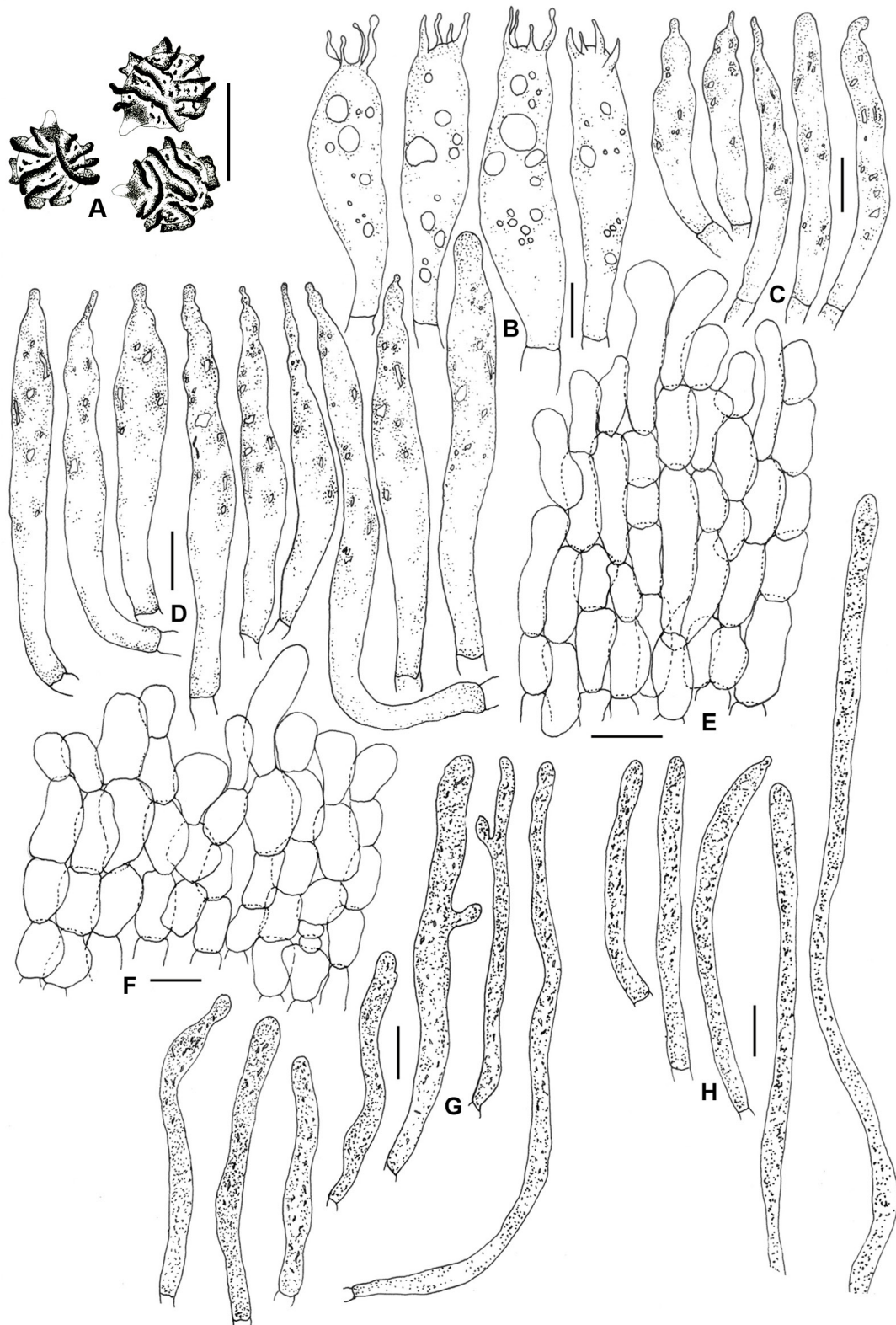


Fig. 6. *Russula pseudosenecis* A.Ghosh, D.Chakr., K.Das & Buyck sp. nov. (from holotype, AG 20-062). **A.** Basidiospores. **B.** Basidia. **C.** Hymenial cystidia near the lamellae edges. **D.** Hymenial cystidia on the lamellae sides. **E.** Hyphal terminations in the pileus center. **G.** Pileocystidia in the pileus center. **F.** Hyphal terminations near the pileus margin. **H.** Pileocystidia near the pileus margin. Scale bars: A–H = 10 μ m.

Basidiospores globose to subglobose, (7.1–)7.5–7.8–8.3(–8.3) × (6.7–)7.0–7.4–7.8(–8.3) μm, Q = (1.02–)1.03–1.06–1.09(–1.13); ornamentation amyloid, composed of up to 2.2 μm high wings running over more or less long distances on the spore surface or even nearly encircling the spores, mixed with a dense, low network of short, laterally flattened, blunt ridges and warts forming an incomplete network, intermixed with crowded, isolated warts and large spines (up to 1.8 μm high), some partly connected; suprahilar spot strongly amyloid, uplifted and distinct; apiculi up to 2.5 μm long. Basidia (40–)46–50–54(–57) × (7–)9–11–13(–14) μm, 4-spored, subclavate to clavate, tapered at the base; sterigmata up to 7 μm long. Hymenial cystidia on lamellae sides (50–)62.4–75.1–87.7(–100) × (6–)6.4–7.8–9.1(–11) μm, abundant, cylindrical to lanceolate with obtuse-rounded, mucronate to capitate or subcapitate, appendiculate to lageniform or moniliform apex, emergent up to 60 μm beyond the basidiole tips, few deeply embedded; content dense, finely crystalline with refractive granular bodies, turning gray-black with sulfovanillin. Lamellae edges fertile with basidia and cystidia. Hymenial cystidia on lamellae edges (34–)37–46.5–56(–60) × 5–6–7(–8) μm, cylindrical to lanceolate with obtuse-rounded, subcapitate to appendiculate apex; content dense, finely crystalline with refractive granular bodies, turning gray-black with sulfovanillin. Marginal cells not differentiated. Subhymenium layer up to 20 μm thick, pseudoparenchymatous. Hymenophoral trama composed mainly of large nests of sphaerocytes and few hyphal elements. Pileipellis orthochromatic in Cresyl Blue, sharply delimited from the underlying sphaerocytes of the context, 120–150 μm thick, two-layered; subpellis 60–75 μm deep, composed of more or less dense, horizontally oriented hyphae and dispersed pileocystidia that originate in the subpellis and not implanted on the top of the suprapellis; suprapellis pseudoparenchymatous, an ixo-palisade, 60–75 μm thick, mainly composed of ascending to erect, densely septate, hyphal terminations composed of inflated or cylindrical cells. Acidoresistant incrustations absent. Hyphal terminations near the pileus margin thin-walled, composed of chains of 3–5 cells; terminal cells (9–)10–13.8–17.7(–26) × (4.5–)6–7.7–9.2(–11) μm, mainly clavate to subglobose, rarely cylindrical, with rounded apex; subterminal cells inflated or cylindrical. Hyphal terminations near the pileus center also thin walled, rarely branched at the subterminal cells; terminal cells slightly longer and less wide, measuring (9–)9.9–15.3–20.6(–25) × (3–)3.5–4.9–6.3(–7) μm, mainly cylindrical or clavate; subterminal cells mainly cylindrical or inflated. Pileocystidia originating from the subpellis only, not as terminal cells in the suprapellis, single-celled, long, flexuous, thin-walled, (50–)53–86.9–121(–150) × (2.5–)3–4.2–5.3(–6) μm, mainly cylindrical, apically mainly obtuse-rounded or mucronate; contents finely crystalline with refractive granular bodies, turning gray-black in sulfovanillin. Pileocystidia in the pileus center slightly shorter (41.6–)42.6–67.6–92.6(–132) × (2–)2.8–4.3–5.8(–5) μm, sometimes with lateral projections, apically obtuse-rounded, otherwise identical. Oleiferous hyphae present. Clamp connections absent from all tissues.

Discussion

Winged basidiospores, i.e., spores that have a well-developed ornamentation that comprises up to 2(–3.5) μm high ridges or crests, some of which are typically running over long distances on the spore surface, are rather exceptional in *Russula*. Such spores have been documented (see Buyck 1989, 1994) for very few, thin-fleshed and often annulate, tropical African species in subg. *Heterophyllidae* sect. *Heterophyllae* sensu Buyck *et al.* (2018), but similar spores are also known from a few northern hemisphere species in sect. *Ingratae* of the same subgenus. Both our new species possess this type of ‘winged’ spore ornamentation, but *R. pseudosenecis* sp. nov. is unique within the entire subgenus in having a strongly amyloid, uplifted suprahilar spot (Figs 4, 5L).

Because of the general field aspect of our new species, there is no hesitation to identify them already at first sight as members of sect. *Ingratae*. This placement was also confirmed by nBLAST of the obtained ITS sequences with top results suggesting strongest similarity to the ‘*R. grata* complex’, principally represented by the European *R. grata* Britzelm. (often still called *R. laurocerasi* Melzer), *R. fragrantissima* Romagn. and *R. illota* Romagn. (Romagnesi 1967). In North America and Asia, these same European

names are still mostly used to refer to endemic, undescribed close relatives or sister taxa, although this situation is now changing in Asia with the recent description by Chen *et al.* (2021) of *R. multilamellulata* B.Chen & J.F.Liang (as “*R. multilamellula*”) and *R. clavula* B.Chen & J.F.Liang (as “*R. clavulus*”). Both Asian species are close relatives of *R. grata* and allies, notwithstanding the fact that their odor was described as “indistinct”; all other species in the ‘*grata*’ lineage develop a unique, strong and sweet smell of bitter almonds, which allows to recognize this complex already when collecting in the field. With the exception of the American *R. mutabilis* Murrill, all of these species possess also a particular type of spore ornamentation consisting of distinctly winged spores for *R. grata* and both new Asian relatives, and a similar but lower ornamentation pattern for the other species.

In Asia, sect. *Ingratae* hosts an additional lineage of species that is absent from North America and Europe. The species of this endemic lineage share the distinctly winged spores with *R. grata* and allies, but these differ from it in the absence of a strong bitter almond smell, which is sometimes replaced by more fetid or disagreeable components. For a very long time this particular pattern (no almond smell but winged spores and poor or disagreeable smell) concerned few species in *Ingratae*. The first was the Chinese *R. punctipes* Singer (Singer 1935), a species that remained ignored ever since, but which was finally rediscovered a few years ago (Song *et al.* 2018). Its look-alike, viz. *R. senecis* Imai, described from Japan hardly a few years later (Imai 1938), was later reported from other Asian countries, although its interpretation must probably be taken ‘sensu lato’ as identifications were not sequenced-based. In India, for instance, specimens identified as *R. senecis* were reported in association with *Vateria indica* L. in the dipterocarp forests of Western Ghats Mountains (Natarajan *et al.* 2005), also from subtropical and temperate deciduous forests under trees of *Quercus* sp. and *Lithocarpus* sp. (Fagaceae Dumort.) in Sikkim Himalaya, India (Das *et al.* 2010) and under *Shorea robusta* in West Bengal (Khatua *et al.* 2015) where it is considered edible and a delicacy by local peoples. The species was also reported from Malaysia peninsula (Chua *et al.* 2012) and Borneo, as well as from Taiwan, Republic of South Korea and from eastern and southern China (<https://inaturalist.ca/taxa/908736-Russula-senecis>). In China, however, it is considered toxic and causing gastro-intestinal intoxications soon after consumption (Chen *et al.* 2014).

Still another wing-spored Asian species that was ignored for many years, viz. *R. guangdongensis* Z.S.Bi & T.H.Li (Bi & Li 1986), might be an earlier name for *R. tsokae* (Das *et al.* 2010), as both share very similar features, including the rare feature of a bright yellow stipe surface. However, sequence data are needed for the Chinese species to confirm this hypothesis.

Today’s generalized use of molecular sequence data in the description of new species clearly suggests now that there exists a whole species complex around *R. senecis* with recent descriptions of *R. subpunctipes* J.Song (Song *et al.* 2020), *R. gelatinosa* Y.Song & L.H.Qiu (Song *et al.* 2018) and now also the here newly described *R. pseudosenecis* sp. nov. and *R. indosenecis* sp. nov. The much smaller *R. benghalensis* (Yuan *et al.* 2020) shares the winged spores and the absence of a bitter almond smell; it is phylogenetically close to – but not part of – the ‘*R. punctipes-senecis*’ complex.

Our new *R. indosenecis* sp. nov. is characterized by a very acrid taste, which is shared only with *R. senecis* and *R. punctipes* among the various species of the same species-complex. The only feature that seems to differentiate it from these two, apart from sequence divergence (showing 97.25%–97.79% similarity with *R. senecis* in nBLAST search), is the singularity of its habitat, being confined so far to trees of subalpine *Abies densa*. *Russula indosenecis* differs from our second new species, *R. pseudosenecis* sp. nov., not only in taste, but also in the less strong amyloidity of the suprahilar spot, and in the structure of its suprapellis which resembles more the typical ‘*virescens*’ type, i.e., composed of strongly inflated, sphaerocyte-like cells at the base that rapidly diminish in diameter toward the terminal cell, while in *R. pseudosenecis* the suprapellis is more dense and composed of less inflated cells that are not so strongly diminishing in diameter toward the terminal cell.

The mild taste of *R. pseudosenecis* sp. nov., for which nrITS sequences are less than 97% similar (for 99% coverage) to any other member of sect. *Ingratae* (i.e., *R. senecis*) allows to distinguish it already in the field from the strongly acrid *R. indosenecis* sp. nov., *R. senecis* and *R. punctipes*. The Chinese *R. guangdongensis* and Indian *R. tsokae*, both equally mild species, differ from the new *R. pseudosenecis* by their distinctly yellow-coloured stipe. This leaves *R. subpunctipes* and *R. gelatinosa*, again two mild species, as most similar species in the field to *R. pseudosenecis*, but all differ morphologically from our species in the lack of the strongly amyloid suprahilar spot. *Russula subpunctipes* develops numerous small reddish punctuations on the stipe and gill edges, reminding the similar, but brownish punctuations of *R. punctipes*, and indeed of our own *R. pseudosenecis*. However, Song *et al.* (2018) suggested that this punctuation might not be a very reliable feature for identification based on their observations on different sequenced collections. As *R. subpunctipes* is known from a single location (two specimens), as indeed most of the sequenced species in the whole *R. senecis* complex, the slight differences – be it in microscopic measurements, in overall size or general colour – should not be given too much importance at this time as they need confirmation based on multiple observations. Detailed documentation of newly sequenced collections will surely help to appreciate the intra- and interspecific variation of these various species much better. Finally, *R. gelatinosa* has repeatedly been suggested as phylogenetically related to the European-North American *R. grata* complex (Song *et al.* 2018; Li *et al.* 2021) and should probably be excluded from the *R. senecis* complex, but multi-locus analyses are needed to confirm its exact affinities.

Acknowledgments

The authors are grateful to the Director of the Botanical Survey of India, Kolkata for providing facilities. Authors (AG and DC) are thankful to Science and Engineering Research Board (SERB) for providing the National Post-Doctoral Research Fellowship (File Nos.: PDF/2021/000183 and PDF/2019/000917 respectively). Dr Manoj E. Hembrom is thanked for assisting AG, DC and IB in the field.

References

- Adamčík S., Looney B., Caboň M., Jančovičová S., Adamčíková K., Avis P.G., Barajas M., Bhatt R.P., Corrales A., Das K., Hampe F., Ghosh A., Gates G., Kälviäinen V., Khalid A.K., Kiran M., De Lange R., Lee H., Lim Y.W., Luz A.K., Manz C., Ovrebo C., Park J.Y., Saba M., Taipale T., Verbeke A., Wisitrasameewong K. & Buyck B. 2019. The quest for a globally comprehensible *Russula* language. *Fungal Diversity* 99 (1): 369–449. <https://doi.org/10.1007/s13225-019-00437-2>
- Bi Z.S. & Li T.H. 1986. A preliminary note on *Russula* species from Guangdong, with a new species and a new variety. *Guihaia* 6 (3): 193–199.
- Buyck B. 1989. Etudes microscopiques de Russules tropicales: *Mimeticinae* subsect. nov. *Mycotaxon* 35: 55–63.
- Buyck B. 1994. *Flore illustrée des Champignons d’Afrique centrale* 16. *Russula II (Russulaceae)* 16: 411–542. Jardin Botanique National de Belgique.
- Buyck B., Zoller S. & Hofstetter V. 2018. Walking the thin line... ten years later: the dilemma of above-versus below-ground features to support phylogenies in the Russulaceae (Basidiomycota). *Fungal Diversity* 89 (1): 267–292. <https://doi.org/10.1007/s13225-018-0397-5>
- Chen B., Song J., Zhang J.-H. & Liang J.-F. 2021. Morphology and molecular phylogeny reveal two new species in *Russula* sect. *Ingratae* from China. *Phytotaxa* 525 (2): 109–123. <https://doi.org/10.11646/phytotaxa.525.2.2>
- Chen Z., Zhang P. & Zhang Z. 2014. Investigation and analysis of 102 mushroom poisoning cases in Southern China from 1994 to 2012. *Fungal Diversity* 64: 123–131. <https://doi.org/10.1007/s13225-013-0260-7>

Chua L.S.L., Lee S.S., Alias S.A., Jones E.G.B., Zainuddin N. & Chan H.T. 2012. *Checklist of Fungi of Malaysia, Issue/No. 132*. Forest Research Institute Malaysia (FRIM), Malaysia.

Crous P.W., Wingfield M.J., Burgess T.I., Hardy G.E.S.J., Barber P.A., Alvarado P., Barnes C.W., Buchanan P.K., Heykoop M., Moreno G., Thangavel R., Van der Spuy S., Barili A., Barrett S., Cacciola S.O., Cano-Lira J.F., Crane C., Decock C., Gibertoni T.B., Guarro J., Guevara-Suarez M., Hubka V., Kolařík M., Lira C.R.S., Ordoñez M.E., Padamsee M., Ryvarden L., Soares A.M., Stchigel A.M., Sutton D.A., Vizzini A., Weir B.S., Acharya K., Aloí F., Baseia I.G., Blanchette R.A., Bordallo J.J., Bratek Z., Butler T., Cano-Canals J., Carlavilla J.R., Chander J., Cheewangkoon R., Cruz R.H.S.F., Da Silva M., Dutta A.K., Ercole E., Escobio V., Esteve-Raventós F., Flores J.A., Gené J., Góis J.S., Haines L., Held B.W., Horta Jung M., Hosaka K., Jung T., Jurjević Ž., Kautman V., Kautmanova I., Kiyashko A.A., Kozanek M., Kubátová A., Lafourcade M., La Spada F., Latha K.P.D., Madrid H., Malysheva E.F., Manimohan P., Manjón J.L., Martín M.P., Mata M., Merényi Z., Morte A., Nagy I., Normand A.-C., Paloi S., Pattison N., Pawłowska J., Pereira O.L., Petterson M.E., Picillo B. & Raj K.N.A. 2017. Fungal Planet description sheets: 558–624. *Persoonia* 38: 240–384. <https://doi.org/10.3767/003158517X698941>

Das K., Sharma J.R. & Atri N.S. 2006. *Russula* in Himalaya 3: A new species of subgenus *Ingratula*. *Mycotaxon* 95: 271–275.

Das K., Van de Putte K. & Buyck B. 2010. New or interesting *Russula* from Sikkim Himalaya (India). *Cryptogamie Mycologie* 31 (4): 373–387.

Das K., Ghosh A., Chakraborty D., Li J., Qiu L., Baghela A., Halama M., Hembrom M.E., Mehmood T., Parihar A., Pencakowski B., Bielecka M., Reczynska K., Sasiela D., Singh U., Song Y., Swierkosz K., Szczesniak K., Uniyal P., Zhang J. & Buyck B. 2017. Fungal Biodiversity Profiles 31–40. *Cryptogamie Mycologie* 38 (3): 1–56. <https://doi.org/10.7872/crym/v38.iss3.2017.353>

Drummond A.J., Ashton B., Buxton S., Cheung M., Cooper A., Heled J., Kearse M., Moir R., Stones-Havas S., Sturrock S., Thierer T. & Wilson A. 2010. Geneious ver. 5.1. Available from <http://www.geneious.com> [accessed 31 Oct. 2022].

Edler D., Klein J., Antonelli A. & Silvestro D. 2021. raxmlGUI 2.0: a graphical interface and toolkit for phylogenetic analyses using RAxML. *Methods in Ecology and Evolution* 12: 373–377. <https://doi.org/10.1111/2041-210X.13512>

Gardes M & Bruns T.D. 1993. ITS primers with enhanced specificity for basidiomycetes-application to the identification of mycorrhizae and rusts. *Molecular Ecology* 2: 113–118. <https://doi.org/10.1111/j.1365-294X.1993.tb00005.x>

Ghosh A., Das K., Bhatt R.P. & Hembrom M.E. 2020. Two new species of the Genus *Russula* from western Himalaya with morphological details and phylogenetic estimations. *Nova Hedwigia* 111 (1–2): 115–130. https://doi.org/10.1127/nova_hedwigia/2020/0588

Ghosh A., Das K. & Buyck B. 2021. Two new species in the *Russula* (Russulaceae, Basidiomycota) crown clade from Indian Himalaya. *European Journal of Taxonomy* 782: 157–172. <https://doi.org/10.5852/ejt.2021.782.1595>

Hackel J., Henkel T.W., Moreau P.-A., De Crop E., Verbeken A., Sà M., Buyck B., Neves M.-A., Vasco-Palacios A., Wartchow F., Schimann H., Carriconde F., Garnica S., Courtecuisse R., Gardes M., Manzi S., Louisanna E. & Roy M. 2022. Biogeographic history of a large clade of ectomycorrhizal fungi, the Russulaceae, in the Neotropics and adjacent regions. *New Phytologist* 236 (2): 698–713. <https://doi.org/10.1111/nph.18365>

Han Y.-X., Liang Z.-Q., Jiang S. & Zeng N.-K. 2022. *Russula hainanensis* (Russulaceae, Russulales), a new species from tropical China. *Phytotaxa* 552 (1): 35–50. <https://doi.org/10.11646/phytotaxa.552.1.3>

- Imai S. 1938. Studies on the Agaricaceae of Hokkaido. II. *Journal of the Faculty of Agriculture of the Hokkaido Imperial University* 43: 179–378.
- Katoh K., Rozewicki R. & Yamada K.D. 2019. MAFFT online service: multiple sequence alignment, interactive sequence choice and visualization. *Briefings in Bioinformatics* 20 (4): 1160–1166. <https://doi.org/10.1093/bib/bbx108>
- Khatua S., Dutta A.K. & Acharya K. 2015. Prospecting *Russula senecis*: A delicacy among the tribes of West Bengal. *PeerJ* 3: e810. <https://doi.org/10.7717/peerj.810>
- Köljalg U., Nilsson R.H., Abarenkov K., Tedersoo L., Taylor A.F.S., Bahram M., Bates S.T., Bruns T.D., Bengtsson-Palme J., Callaghan T.M., Douglas B., Drenkhan T., Eberhardt U., Dueñas M., Grebenc T., Griffith G.W., Hartmann M., Kirk P.M., Kohout P., Larsson E., Lindahl B.D., Lücking R., Martín M.P., Matheny P.B., Nguyen N.H., Niskanen T., Oja J., Peay K.G., Peintner U., Peterson M., Pöldmaa K., Saag L., Saar I., Schüßler A., Scott J.A., Senés C., Smith M.E., Suija A., Taylor D.L., Telleria M.T., Weiss M. & Larsson K.-H. 2013. Towards a unified paradigm for sequence-based identification of Fungi. *Molecular ecology* 22: 5271–5277. <https://doi.org/10.1111/mec.12481>
- Kornerup A. & Wanscher J.H. 1978. *Methuen Handbook of Colour, 3rd Edition*. Methuen, London.
- Lanfear R., Frandsen P.B., Wright A.M., Senfeld T. & Calcott B. 2017. PartitionFinder 2: new methods for selecting partitioned models of evolution for molecular and morphological phylogenetic analyses. *Molecular Biology and Evolution* 34 (3): 772–773. <https://doi.org/10.1093/molbev/msw260>
- Li G.-J., Li S.-M., Buyck B., Zhao S.-Y., Xie X.-J., Shi L.-Y., Deng C.-Y., Meng Q.-F., Sun Q.-B., Jun-Qing Yan J.-Q., Wang J. & Li M. 2021. Three new *Russula* species in sect. *Ingratae* (Russulales, Basidiomycota) from southern China. *MycKeys* 84: 103–139. <https://doi.org/10.3897/mycokeys.84.68750>
- Natarajan K., Senthilrasu G., Kumaresan V. & Riviera T. 2005. Diversity in Ectomycorrhizal fungi of a dipterocarp forest in Western Ghats. *Current science* 88 (12): 1893–1895.
- Romagnesi H. 1967. *Les Russules d'Europe et d'Afrique du Nord*. Bordas, Paris.
- Rambaut A., Suchard M.A., Xie D., & Drummond A.J. 2014. Tracer version 1.6. Available from <http://beast.bio.ed.ac.uk/tracer> [accessed 31 Oct. 2022].
- Ronquist F., Teslenko M., van der Mark P., Ayres D.L., Darling A., Höhna S., Larget B., Liu L., Suchard M.A. & Huelsenbeck J.P. 2012. MrBayes 3.2: efficient Bayesian phylogenetic inference and model choice across a large model space. *Systematic Biology* 61: 539–542. <https://doi.org/10.1093/sysbio/sys029>
- Sarnari M. 1998. *Monografia Illustrata del Genere Russula in Europa, Prima Parte*. Associazione Micologica Bresadola, Trento.
- Singer R. 1935. *Supplemente zu meiner Monographie der Gattung Russula. Annales Mycologici* 33: 297–352.
- Singer R. 1986. *The Agaricales in Modern Taxonomy. 4th Edition*. Koeltz Scientific Books, Koenigstein.
- Song J., Chen B., Liang J.-F., Li H.-J., Wang S.-K. & Lu J.-K. 2020. Morphology and phylogeny reveal *Russula subpunctipes* sp. nov., from southern China. *Phytotaxa* 459 (1): 016–024. <https://doi.org/10.11646/phytotaxa.459.1.2>
- Song Y., Buyck B., Li J.W., Yuan F., Zhang Z.W. & Qiu L.H. 2018. Two novel and a forgotten *Russula* species in sect. *Ingratae* (Russulales) from Dinghushan Biosphere Reserve in southern China. *Cryptogamie, Mycologie* 39: 341–357. <https://doi.org/10.7872/crym/v39.iss3.2018.341>
- Vellinga E.C. 1988. Glossary. In: Bas C., Kuyper T.H.W., Noordeloos M.E. & Vellinga E.C. (eds) *Flora Agaricina Neerlandica, Supplemente zu meiner Monographie der Gattung Russula Vol. 1*. A.A. Balkema, Rotterdam. Netherlands.

White T.J., Bruns T., Lee S.S. & Taylor J. 1990. Amplification and direct sequencing of fungal ribosomal RNA genes for phylogenetics. In: Innis M.A., Gelfand D.H., Sninsky J.J. & White T.J. (eds) *PCR Protocols: a Guide to Methods and Applications*: 315–322. Academic Press, New York. <https://doi.org/10.1016/B978-0-12-372180-8.50042-1>

Yuan H.-S., Lu Xu., Dai Yu.-C., Hyde K.D., Kan Yu.-H., *et al.* 2020. Fungal diversity notes 1277–1386: taxonomic and phylogenetic contributions to fungal taxa. *Fungal Diversity* 104: 1–266.

Manuscript received: 1 April 2022

Manuscript accepted: 21 September 2022

Published on: 28 November 2022

Topic editor: Frederik Leliaert

Desk editor: Radka Rosenbaumová

Printed versions of all papers are also deposited in the libraries of the institutes that are members of the *EJT* consortium: Muséum national d’histoire naturelle, Paris, France; Meise Botanic Garden, Belgium; Royal Museum for Central Africa, Tervuren, Belgium; Royal Belgian Institute of Natural Sciences, Brussels, Belgium; Natural History Museum of Denmark, Copenhagen, Denmark; Naturalis Biodiversity Center, Leiden, the Netherlands; Museo Nacional de Ciencias Naturales-CSIC, Madrid, Spain; Leibniz Institute for the Analysis of Biodiversity Change, Bonn – Hamburg, Germany; National Museum, Prague, Czech Republic.